DRA-47. IN SITU DIRECT SHEAR TESTS OF THE QUESTA MINE ROCK PILES AND ANALOG MATERIALS

K. Boakye, A. Fakhimi, and V.T. McLemore, May 9, 2007, revised February 16, 2009 (reviewed by Navid Mojtabai, D. van Zyl)

1. STATEMENT OF THE PROBLEM

What is the extent of cementation and cohesion of the Questa rock pile materials? Does correlation exist between the cohesion and friction angle with the degree of weathering and age of the rock piles and analogs (alteration scar and debris flow)? Cohesion and friction angle are important parameters in controlling the gravitational stability of the Questa rock piles.

2. PREVIOUS WORK

A comprehensive geotechnical characterization of the mine rock piles has been carried out at the Questa site over the last few years to evaluate their current characteristics. The majority of previous tests for determining the rock-piles strength parameters were performed in laboratories. Gutierrez (2006) performed laboratory direct shear tests, using 2- and 4-inch shear boxes, to determine the internal friction angles of the air-dried samples from Goathill North (GHN) rock pile, and reported a peak friction angle range of 40° to 47° and a residual friction angle range of 37° to 41°. In the front rock piles, Norwest Corporation (2005) reported a range of internal friction angle values close to those of Gutierrez (2006). Azam and Wilson (2006) performed shear tests on rock-pile samples and reported peak and residual friction angles that were in general lower than those reported by Gutierrez (2006). This could be a result of testing saturated samples by Azam and Wilson (2006). Note also Gutierrez (2006) reported the friction angles assuming the failure envelopes passed through the origin, i.e. zero cohesion was assumed in her analyses.

The majority of the shear tests in the previous studies were performed on dry specimens assuming cohesion of 0 for the rock-pile material. However, cohesion exists due to matric suction and cementation (El-Sohby et al., 1987; Pereira, 1996; Pereira and Fredlund, 1999), and should be measured. Intact samples can be collected and tested in the laboratory, but the Questa rock-pile material contains large pieces of rock and boulders that make it difficult to collect undisturbed specimens. Disturbed specimens might not be completely representative of original field specimens. To obtain more reliable shear strength parameters of the rock-pile material, an in-situ shear apparatus was designed similar in configuration to the one used by Fakhimi et al. (2004). In-situ shear testing has been used successfully in the past by several authors to evaluate soil or rock-pile shear strength (O'Loughlin et al., 1976, Matsuoka et al. 2002, Brand et al. 1983, and Lui et al., 2004).

3. TECHNICAL APPROACH

An in-situ shear test apparatus was designed at NMIMT and fabricated by Questa mine engineers. The apparatus consists of a 30-cm or 60-cm square metal shear box, a metal top plate, a fabricated roller plate, normal and shear dial gages with wooden supports, and two hydraulic jacks. Unlike conventional laboratory shear and in-situ shear test

apparatuses that consist of two boxes that move relative to each other, the in-situ shear box designed for this project is made of only one box. This innovation allows for easier and faster site preparation. Further details about this box, its accessories, and the procedures employed to conduct the in-situ direct shear test are in Fakhimi et al. (2008) and Boakye (2008).

In-situ tests were performed on both rock piles and natural weathering analogs. Areas of alteration scars and debris flows near the Questa mine have been identified as natural weathering analogs to the mineralogical changes in the rock piles expected during long-term weathering (Ludington et al., 2005; Campbell and Lueth, 2008; Graf, 2008). Note that the weathering processes operating in the natural analogs share many similarities to those in the rock piles, although certain aspects of the physical and chemical systems are different (DRA-19, 20, 22). Boakye (2008) and Appendix 1 describe in detail the natural analogs and the comparison between the rock piles and their natural analogs. In-situ direct shear tests were performed on these natural analogs to extrapolate the future shear strength of the rock piles. The in-situ test locations were selected based on geologic characteristics (weathering and cohesion), personnel safety factors, and easy accessibility for the equipment (DRA-47a). The applied normal stress for the in-situ tests ranges from 15 to 75 kPa. Measurements of matric suction and soil temperature were taken at the shear plane following the appropriate standard operating procedures (SOPs). Representative samples were sent to the laboratory for Atterberg limits, specific gravity, and disturbed laboratory direct-shear tests, plus moisture content, particle size, mineralogical, chemical, and petrographic analyses. After each in-situ shear test, the shear plane was inspected for the maximum particle size and was photographed. Particle size analyses were performed in the laboratory on the rock-pile samples that were collected from the in-situ test locations. A total of 52 in-situ shear tests were conducted at 13 locations as shown in Table 1 and located in Figure 1.

TABLE 1. The number of in-situ direct shear tests performed at each location.

Location	**Number of in-situ direct shear tests performed**	**Number in Figure 1 (Test site identification number)**
Middle Rock Pile	5	MID1 (MID-AAF-1-1, 2-1, 2-2, 3-1) MID2 (MID-VTM-0002-1)
Spring Gulch Rock Pile	10	SPR1 (SPR-AAF-0001-1, 1-2) SPR2 (SPR-VTM-0005-1, 8-1) SPR3 (SPR-VTM-0012-1, 12-2, 12-3, 19-1, 19-2)
Sugar Shack South Rock Pile	7	SSS1 (SSS-AAF-0001-1, 5-1, 5-2, 9-1, 9-2) SSS2 (SSS-VTM-0600-1, 601-1)
Sugar Shack West Rock Pile	17	SSW1 (SSW-AAF-0001-1, 2-1, 2-2, 2-3, 4-1) SSW2 (SSW-AAF-0005-1, 7-1) SSW3 (SSW-VTM-0016-1, 16-2, 23-1, SSW-VTM-0600-1, 600-2, 600-3) SSW4 (SSW-VTM-0026-1, 26-2, 30-1, 30-2)
Questa Pit Alteration Scar	8	QPS (QPS-AAF-0001-1, 1-2, 1-3, 8-1, 9-1, 20-1, 22-1, QPS-VTM-0001-1)
Debris Flow	5	MIN (MIN-AAF-0001-1, 4-1, 10-1, 12-1, 15-1)

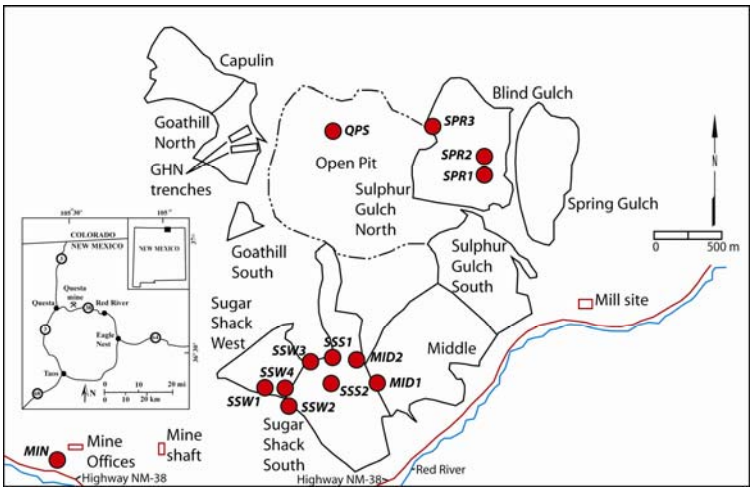

FIGURE 1. Location of in-situ samples (red circles). Test site identification numbers are listed in Table 1.

It is difficult, but possible, to distinguish between pre-mining hydrothermal alteration and post-mining weathering by using detailed field observations and petrographic analysis that includes defining the paragenesis (sequence of events), especially using microprobe analyses (DRA-27; McLemore et al. 2008a, b). Characterization of the in-situ test samples is described in McLemore and Dickens (2008b). Numerous weathering indices were evaluated for their applicability in the Questa rock piles (McLemore et al., 2008b). A weathering index is a measure of how much the sample has weathered. A simple weathering index (SWI) was developed to differentiate the weathering intensity of Questa rock-pile materials (McLemore et al., 2008a, b). Five classes (Table A2-1) describes the SWI classification for the mine soils at the Questa mine based on relative intensity of both physical and chemical weathering (SWI=1, least weathered to SWI=5, most weathered; modified in part from Little, 1969; Gupta and Rao, 1998; Blowes and Jambor, 1990). The determination of relative intensity is based on the surface character of the larger rock fragments and the soil matrix; the interior of the rock fragments can be unweathered even though the surface and surrounding matrix is weathered. The Questa Mineralogical Weathering Index is a quantified index that ranges from 0-7 and accounts for changes in the pyrite-calcite-gypsum system that is the most predominant weathering system at Questa (DRA-16; McLemore et al., 2008b). Other indices or parameters that can be used to indicate some aspects of weathering in the Questa rock piles include paste pH, authigenic gypsum, sum of gypsum and jarosite, SO_4, slake durability index, point load index, and net NP (neutralizing potential; McLemore et al., 2008b).

4. CONCEPTUAL MODEL

The matric suctions that were measured in the field using a tensiometer, ranged between 0 to 45 kPa for all 52 in situ test locations. Cohesion is composed of three components, matric suction, cementation, and interlocking of grains. To obtain the cohesion parameters for the same values of matric suction, the modified Mohr-Coulomb failure criterion (Eqs. 1a to 1c) was used (Fredlund and Rahardjo, 1993)

$$\tau = c + (\sigma - u_a)\tan\varphi \qquad (1a)$$

$$c' = c - (u_a - u_w)\tan\varphi^b \quad (1b)$$
$$c'' = c' + (u_a - u_w)\tan\varphi^b \quad (1c)$$

where τ and σ are shear and normal stresses, u_a and u_w are air and pore water pressures, c and φ are cohesion and friction angle, and φ^b is the angle that dictates the increase in cohesion due to the increase in matric suction, $(u_a - u_w)$. With u_a equal to zero, an assumed φ^b of 15º (Fredlund and Rahardjo, 1993), the cohesion *c* in Eq. (1b) can be used to find the cohesion *c′* for zero suction. Eq. 1c is then can be used to obtain the cohesion corresponding to a given matric suction (*c″*).

5. STATUS OF COMPONENT INVESTIGATIONS

The rock piles and analogs sampled at all 52 in-situ test locations consisted of heterogeneous material made up of 32% to 80% gravel, 16% to 66% sand, and 0.1% to 14% fines. These values correspond relatively well with those of Gutierrez (2006), Shaw et al. (2002), and Norwest Corporation (2005). The Atterberg limits range from 19 to 40 for liquid limit, 13 to 32 for plastic limit, and 0.2 to 19 for plasticity index. Based on this information, the Questa rock-pile materials are classified as GP-GM to SP-SC using the Unified Soil Classification System. Figure A3-1 of Appendix 3 shows the gradation curves of the materials at the in-situ tests locations.

The main purpose for performing in-situ shear tests was to measure the rock-pile cohesion to investigate the intensity of cementation between particles. For this reason, in some rock piles, a few shear tests at different locations were conducted with identical low normal stresses. Therefore, in order to obtain the cohesion, the normal stress-peak shear stress from an in-situ test and the corresponding laboratory friction angle were used together with the Mohr-Coulomb failure envelope. The laboratory friction angles were obtained by conducting direct shear tests on dry specimens compacted to the in-situ dry density using low normal stresses in the range of 20 to 110 kPa. The laboratory shear box was 2-inch in width (DRA-42) and used to test materials that passed sieve No. 6. Table A3-1 (Appendix 3) reports some geotechnical parameters of the rock piles and analogs such as % fine, PI, matric suction, and cohesion at the 24 locations where successful in-situ shear tests were conducted. A valid or successful shear test was defined as the one that the largest rock fragment in the shear block was smaller than one fifth of the box width (refer to DRA-48 for the selection of one fifth). In Table A3-1, means and standard deviations of cohesions corresponding to the fixed SWI values (Simple Weathering Index, Appendix 2) are shown as well. The cohesion values range between 0 to 46.1 kPa.

Figures 2 and A3-2 (Appendix 3) show the results of field-measured cohesions versus the simple weathering index. The averaged cohesion corresponding to each weathering index is shown in Figure A3-2 with a gray circle. Figures 2 and A3-2 suggests that higher cohesion values belong to more weathered samples, but there are some weathered samples with low cohesion values.

Table A3-2 (Appendix 3) reports the mean and standard deviation for cohesion of the rock piles and analogs separately. In order to evaluate the trend in cohesion change with time, t-tests were performed using the data in Table A3-2 and Figure A3-3 (Appendix 3) that shows the cohesion versus time. Since the rock piles were constructed using the end-dumping method with no mechanical compaction, it is reasonable to assume the cohesion of these materials was near 0 at the time of construction. With this assumption, before and after pair t-tests were conducted to investigate the improvement

in cohesion since the rock piles placement. The improvement in the mean of cohesion with a 95% confidence was between 6.2 to 13.1 kPa. Another t-test between the rock piles at the current situation and their natural analogs indicated that the present mean cohesion of the rock piles of 9.6 kPa, in future will improve with 95% confidence to a value between 18.6 to 38.2 kPa. Note that the results of these two t-tests are approximate for the following reasons:

- The number of data points, 20 cohesion values for the rock piles and 4 cohesion values for the analogs do not represent enough samples (especially for the analogs) to be statistically significant.
- The measured cohesions on the rock piles belong to the locations where a shear test block could be made i.e. the locations that the rock piles had cohesion. There were several locations where a shear block could not be made to run the shear test because of lack of or low cohesion. Therefore, the shear tests on the rock pile are biased toward to the locations where cohesion exists.
- The statistical distribution of the cohesion values must be normal for the t-tests to be accurate.

In-situ direct shear test results indicate that cohesion exists locally within the rock piles. Higher values of cohesion are associated with the debris flow sites. The evidence of cohesion in the Questa rock piles is due to the presence of:

- Clay pockets within the rock piles and analog sites
- Jarosite, gypsum, Fe-oxide cementing minerals, and soluble efflorescent salts
- Matric suction
- Interlocking of grains.

Figure A3-4 (Appendix 3) illustrates the friction angle versus the SWI for the 52 samples collected from the in-situ test sites. The laboratory friction angles in Figure A3-4 were obtained using two sets of normal stresses. In the first set, low normal stresses of 20 to 110 kPa was used, while for the second set the normal stresses were higher (150 to 650 kPa). The majority of the samples in Figure A3-4 were compacted at the in-situ dry densities but there are some samples which were not compacted at the in-situ dry densities; the range of dry densities used for sample compaction was 1410 to 2170 kg/m^3 (Table A3-3). As expected, on average, the friction angles obtained from shear tests with low normal stresses are higher than those obtained from shear tests with high normal stresses. This indicates that a curved failure envelope can be used to capture the shear strength of the rock pile material (Boakye, 2008; Boakye et al., in preparation). Note that two friction angles from the in-situ shear tests were measured and are shown in Figure A3-4.

Previous studies showed a decrease in friction angle of some of the weathered samples (but not all) from the surface layer of the rock piles due to weathering (Gutierrez, 2006; Gutierrez et al., 2008). The mean and standard deviation of friction angles corresponding to the high normal stress range for simple weathering indices of 2, 3, 4, 5 are (41.0°, 4.2°), (42.8°, 3.3°), (42.0°, 4.1°), (38.7°, 3.2°), respectively. Note that the laboratory friction angles from the in-situ tests locations do not indicate any significant change in friction angle with increase in weathering except for the samples with SWI of 5 that show in average 2 to 3 degrees reduction in friction angle. On the other hand, this change in friction angle is within the range of scatter of the data and may not indicate reduction of friction angle with the weathering that so far has occurred in these samples.

To exclude the effect of compaction density on the measured peak friction angles, in Figures A3-5 and A3-6 the peak friction angles are plotted versus the simple weathering index and time for only 32 samples with compacted laboratory dry densities within 0.95 to 1.05 of the corresponding in situ dry densities. These samples are shown in gray in Table A3-3. These two figures suggest that the mean friction angle is not noticeably affected by the weathering for the in-situ test locations. In particular, Figure A3-6 indicates that the mean friction angle of rock piles and analogs are close to each other and they show similar scatter of the data as well.

Note that in general the mean friction angles are above 40º. The high friction angles of the rock piles are due to the following reasons:

- The percentage of fine material is low (less than 20%, Fig. A3-1, Appendix 3). This allows the rock fragments in the rock piles to be directly in contact and, therefore, have more frictional resistance.
- Rock fragments at the Questa mine are highly durable. For example, the slake durability index for 90 samples from GHN rock pile ranged from 82 to 98% (DRA-46; Viterbo, 2007; Gutierrez et al., 2008). These samples are classified as being high to extremely high durable based on Franklin's durability classification. (Franklin and Chandra, 1972). However, Viterbo (2007) and Gutierrez et al. (2008) showed slake durability index of the GHN rock pile samples decreased as the degree of weathering increased in some samples but not all.
- The rock fragments in the rock piles have relatively high compressive and tensile strengths. For example, test results on rock fragments from GHN rock pile showed point load strength in the range of 0.6 to 8.2 MPa (DRA-46). These samples are classified with medium to very high strength according to Broch and Franklin (1972). The medium to very high strength of the rock fragments prevents particle breakage during a shear test, especially at low normal stresses, which causes greater frictional resistance of the material. However, Viterbo (2007) and Gutierrez et al. (2008) showed that the point load strength index of the GHN rock pile samples decreased as the degree of weathering increased in some samples but not all.
- The rock fragments in the rock piles are angular to subangular. Angularity causes greater interlocking of the particles and induces higher shearing resistance. The angularity of the rock fragments (DRA-28) is shown in Figure A3-7 (Appendix 3).

In addition to the simple weathering index, Questa Mineralogic Weathering Index (QMWI; Figure A2-2 in Appendix 2), paste pH, sum of gypsum and jarosite, SO_4 and $SO_4/(S+ SO_4)$,were used in this investigation (DRA-27; Appendix 2). These were confirmed by petrographic analysis (McLemore et al., 2008a, b). The correlation between these parameters with cohesion values are shown in Figure 2 in which different symbols for the rock piles, alteration scar, and debris flow are being used. Some samples that are weathered (i.e. high SWI, QMWI, SO_4 and $SO_4/(S+ SO_4)$, and low paste pH) have high cohesion, but not all.

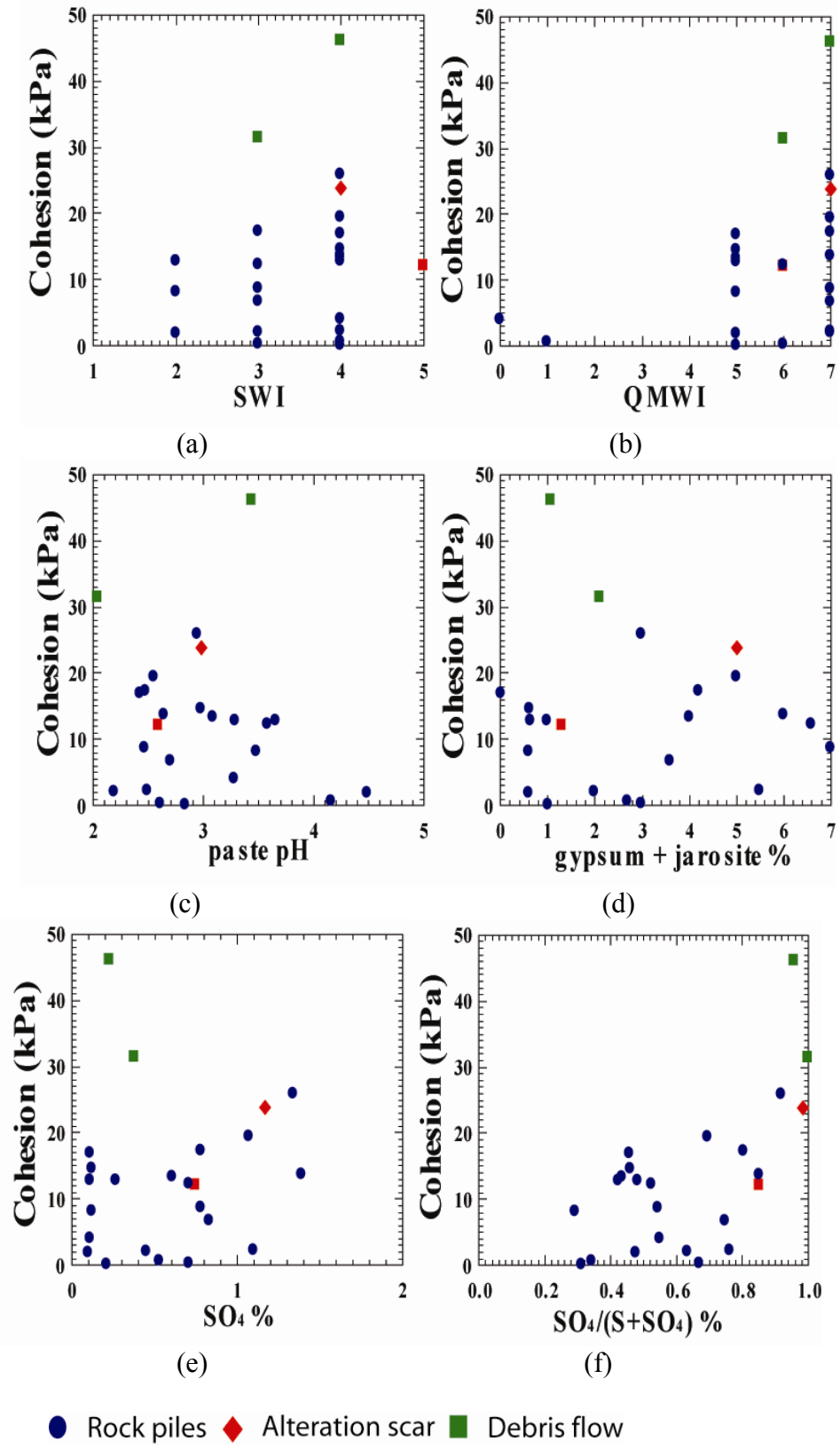

FIGURE 2. Scatter plot of cohesion vs. SWI (Simple Weathering Index), QMWI (Questa Mineralogic Weathering Index), paste pH, gypsum + jarosite, SO_4 and $SO_4/(S+ SO_4)$.

Some samples that are weathered (i.e. high SWI, QMWI, SO_4 and $SO_4/(S+ SO_4)$, and low paste pH) have high cohesion, but not all.

In Figure A3-8 (Appendix 3), the cohesion values corresponding to 0 matric suction (c' in equation 1b) versus SWI are shown. This figure suggests that the greatest cohesion values belong to more weathered samples but there are weathered samples with low cohesion values too.

6. RELIABILITY ANALYSIS

There are some uncertainties associated with the measured cohesions and friction angles. The in-situ tests were conducted on the rock-pile surfaces at the locations where the shear block could be constructed. Therefore, the results are biased toward locations where cementation exists. Furthermore, the number of in-situ shear tests may not be statistically significant to provide full confidence on the results of the t-tests conducted in the previous section of this DRA. It should be noted that all the in-situ shear tests were performed on the top surface layers of the rock piles, and the conclusions presented are valid only for these portions of the rock piles. Further investigation and testing are required at greater depths into the rock piles.

7. CONCLUSIONS OF THE COMPONENT

Laboratory and in-situ direct shear tests were conducted on the Questa rock-pile materials to investigate the effect of weathering and time on the shear strength of these materials. The in-situ shear tests results are summarized as follows:

- In general, the majority of rock-pile samples have high peak friction angles (40° or above) even after having undergone hydrothermal alteration and blasting prior to deposition and after subsequent exposure to weathering for approximately 25-40 years (DRA-42; Gutierrez, 2006; Viterbo, 2007; Gutierrez et al., 2008).
- The peak friction angle of the rock piles and their analogs show similar mean values. The scatter of the data is similar for the friction angles of the rock piles and analogs as well. These observations suggest that the weathering of the material has not caused noticeable reduction in the friction angle at the in-situ test locations.
- There is a statistically significant difference (using a one way ANOVA, analysis of variance) in cohesion between the alteration scar, debris flow, and Questa rock piles ($P = <0.001$); the alteration scar (2 samples) and debris flow (2 samples) have higher cohesion values than the rock piles (20 samples) (Appendix 4). Additional tests are required to confirm this conclusion. Higher cohesion values correspond to the alteration scar and debris flow samples that are older than the rock piles.
- To classify the rock-pile material based on the weathering intensity, several parameters indicating weathering were used. These were confirmed by petrographic analysis. Some samples that are weathered (i.e. high SWI, QMWI, SO_4 and $SO_4/(S+ SO_4)$) have high cohesion, but not all. In fact there are some weathered samples with very low cohesion. The increased cohesion of some samples is likely due to post-deposition oxidation, and is consistent with the change in color of the oxidized sample, chemical classification as potential acid-forming (Fig. A2-1, Appendix 2; DRA-7a), loss or obscuring of original igneous texture on the edges and within many rock fragment grains, and increase in

weathered minerals within the in-situ samples (i.e. gypsum, jarosite, and Fe-oxide minerals).

- If the debris flow and alteration scar are analogs for the rock piles, with 95% confidence, the current mean cohesion of the rock piles will increase with time. This increase of cohesion with time is attributed to the gradual compaction of the rock piles and the presence of cementing agents like jarosite, gypsum, pre-existing clay minerals, Fe-oxide minerals, and soluble efflorescent salts in the rock piles.

8. REFERENCES CITED

Ayakwah, G., Dickens, A., and McLemore, V.T., 2008, Characterization of a debris flow profile, Questa, New Mexico: revised unpublished report to Molycorp Task B1.4.

Azam, S., and Wilson, G. W., 2006, Geotechnical characterization of shear strength and hydraulic properties of waste rock samples from Questa Mine, Norman B. Keevil Institute of Mining Engineering, University of British Columbia, Vancouver, British Columbia, Canada.

Blowes, D.W. and Jambor, J.L., 1990, The pore-water geochemistry and the mineralogy of the vadose zone of sulphide tailings, Waite Amulet, Quebec, Canada: Applied Geochemistry, v. 5, p. 327-346.

Brand, E.W., Phillipson, H.B., Borrie, G.W., and Clover, A.W., 1983, In situ shear tests on Hong Kong residual soils. In Proceedings of the Symposium International In-Situ Testing volume 2, Paris, p. 13-17.

Broch, E. and Franklin, J. A., 1972, The Point Load Strength Test: International Journal of Rock Mechanics and Mineral Sciences, v. 9, p. 669-697.

Boakye, K., 2008, Large in situ direct shear tests on rock piles at the Questa Mine, Taos County, New Mexico: M.S. thesis, New Mexico Institute of Mining and Technology, Socorro, 156 p.

Boakye, K., Fakhimi, A., and McLemore V.T., in preparation, Comparison of the in situ and laboratory shear test results on Questa rock pile material.

Campbell A.R., and Lueth V.W., 2008, Isotopic and textural discrimination between hypogene, ancient supergene, and modern sulfates at the Questa Mine, New Mexico: Applied Geochemistry, v. 23, p. 308-319.

El-Sohby, M.A., El-Khoraibi, M.C., Rabba, S.A., and El-Saadany, M.M.A., 1987, Role of soil fabric in collapsible soils: Proceedings, VIII PCSMFE, Cartagena, Columbia, p. 9-20.

Fakhimi, A., Salehi, D., and Mojtabai, N., 2004, Numerical back analysis for estimation of soil parameters in the Resalat Tunnel project: Tunneling and Underground Space Technology, v. 19, p. 57-67.

Fakhimi A., Boakye K., Sperling D., and McLemore V., 2008, Development of a modified in situ direct shear test technique to determine shear strength of mine rock piles: Geotechnical Testing Journal, v. 31, no. 3, paper on line www.astm.org

Franklin, J.A., Chandra, A., 1972, The slake durability test: International Journal of Rock Mechanics and Mining Science, v. 9, p. 325–341.

Fredlund, D.G., and Rahardjo, H., 1993, Soil Mechanics for Unsaturated Soils: Wiley.

Graf, G.J., 2008, Mineralogical and geochemical changes associated with sulfide and silicate weathering, natural alteration scars, Taos County, New Mexico: M. S. thesis, New Mexico Institute of Mining and Technology, Socorro, 193 p., http://geoinfo.nmt.edu/staff/mclemore/Molycorppapers.htm, accessed April 28, 2008.

Gupta, A.S. and Rao, K.S., 1998, Index properties of weathered rocks: inter-relationships and applicability: Bulletin Engineering Geology and Environment, v. 57, p. 161-172.

Gutierrez, L.A.F., 2006, The influence of mineralogy, chemistry and physical engineering properties on shear strength parameters of the Goathill North rock pile material, Questa Molybdenum Mine, New Mexico: M.S. thesis, New Mexico Institute of Mining and Technology, Socorro, 201 p.,http://geoinfo.nmt.edu/staff/mclemore/Molycorppapers.htm, accessed November 19, 2006.

Gutierrez, L.A.F., Viterbo, V.C., McLemore, V.T., and Aimone-Martin, C.T., 2008, Geotechnical and Geomechanical Characterisation of the Goathill North Rock Pile at the Questa Molybdenum Mine, New Mexico, USA; *in* Fourie, A., ed., First International Seminar on the Management of Rock Dumps, Stockpiles and Heap Leach Pads: The Australian Centre for Geomechanics, University of Western Australia, p. 19-32.

Little, A. L., 1969, The engineering classification of residual tropical soils; *in* Za-Chieh Moh, ed., Proceedings of the 7th International Conference on soil mechanics and foundation engineering, Mexico: Asian Institute of Technology, v. 1, p. 1-10.

Ludington, S., Plumlee, G., Caine, J., Bove, D., Holloway, J., and Livo, E., 2005, Questa baseline and pre-mining ground-water quality Investigation, 10. Geologic influences on ground and surface waters in the lower Red River watershed, New Mexico: U.S. Geological Survey, Scientific Investigations Report 2004-5245, 46 p.

Lui., S. H., Xiao, G. Y., Yang, J. Z., and Wu, G. Y., 2004, Large-Scale In-situ Direct Shear Test on Rockfill Materials of Upper Reservoir Dam, *in* eds, Wieland, R. and Tan, Y. Pumped Storage Power Station: Taylor and Francis Group, London ISBN 04 1536 240 7

Matsuoka, H., Lui, S., Sun, D., and Nishikata, U., 2002, Discussion on Development of a New In-situ Direct Shear Test: Geotechnical Testing Journal, v. 25, no. 3. p. 1.

McLemore, V.T., 2008, Evaluation of weathering indices for the Questa rock piles: unpublished report to Chevron, Task B1.1.

McLemore, V.T., Boakye, K., Campbell, A., Donahue, K., Dunbar, N., Gutierrez, L. Heizler, L., Lynn, R., Lueth, V., Osantowski, E., Phillips, E., Shannon, H., Smith, M. Tachie-Menson, S., van Dam, R., Viterbo, V.C., Walsh, P., and Wilson, G.W., 2008a, Characterization of Goathill North Rock Pile: revised unpublished report to Molycorp, Tasks: 1.3.3, 1.3.4, 1.4.2, 1.4.3, 1.11.1.3, 1.11.1.4, 1.11.2.3, B1.1.1, B1.3.2.

McLemore, V.T. and A. Dickens, 2008a, Petrographic Analysis, Mineralogy, and Chemistry of Samples Analyzed by In-Situ Direct Shear Methods, Questa, New Mexico: report to Chevron, Task B1.

McLemore, V.T. and A. Dickens, 2008b, Petrographic Analysis, Mineralogy, and Chemistry of Samples Analyzed by In-Situ Direct Shear Methods, Questa, New

Mexico: report to Chevron, Task B1.McLemore, V.T., Donahue. K.M., Phillips, E., Dunbar, N., Walsh, P., Gutierrez, L.A.F., Tachie-Menson, S., Shannon, H.R., Wilson, G.W., and Walker, B.M., 2006a, Characterization Of Goathill North Mine Rock Pile, Questa Molybdenum Mine, Questa New Mexico, *in* National Meeting of the 7th ICARD, SME, and American Society of Mining and Reclamation: St. Louis, Mo., March, CD-ROM

McLemore, V.T., Donahue. K. M., Phillips, E., Dunbar, N., Smith, M., Tachie-Menson, S., Viterbo, V., Lueth, V. W., Campbell, A. R., and Walker, B. M., 2006b, Petrographic, mineralogical and chemical characterization of Goathill North Mine Rock Pile, Questa Molybdenum Mine, Questa New Mexico: Billings Land Reclamation Symposium, June, 2006, Billing, Mt. Published by American Society of Mining and Reclamation, 3134 Montavesta Rd., Lexington, KY CD-ROM

McLemore, V.T., Donahue, K., Dunbar, N. and Heizler, L., 2008b, Characterization of physical and chemical weathering in the rock piles and evaluation of weathering indices for the Questa rock piles: unpublished report to Chevron, Task 1.3, B1.1

Norwest Corporation, 2005, Questa Roadside Rockpiles 2005 Operation Geotechnical Stability Evaluation: unpublished report to Molycorp Inc., 210 p., 3 vol.

O'Loughlin, C.L. and Pearce, A.J., 1976, Influence of Cenozoic geology on mass movement and sediment yield response to forest removal, North Westland, New Zealand: Bulletin of the International Association of Engineering Geology, v. 14, p. 41-46.

Pereira, J.H.F., 1996, Numerical analysis of the mechanical behavior of collapsing earth dams during first reservoir filling: PhD dissertation, University of Saskatchewan, Saskatoon, Saskatchewan, Canada, 449 p.

Pereira, J. H. F. and Fredlund, D. G., 1999, Shear strength behavior of a residual is of gneiss compacted at metastable-structured conditions, *in* Proceedings of the 11th Pan American Conference on Soil Mechanics and Geotechnical Engineering: Iguanzu Falls, Brazil, v. 1, p. 369-377.

Shaw, C.W., Robertson, A.W., and Lorinczi, G., 2002, Physical and Geochemical Characterization of Mine Rock Piles at the Questa Mine, New Mexico: http://www3.interscience.wiley.com/cgibin/abstract/105556913/ABSTRACT?CRETRY=1&SRETRY=0, accessed April 18, 2007.

Tachie-Menson, S., 2006, Characterization of the acid-Producing potential and investigation of its effect on weathering of the Goathill North Rock Pile at the Questa Molybdenum Mine, New Mexico: M.S. thesis, New Mexico Institute of Mining and Technology, Socorro, NM, 209 p., http://geoinfo.nmt.edu/staff/mclemore/Molycorppapers.htm, accessed March 31, 2008.

Viterbo, V.C., 2007, Effects of pre-miming hydrothermal alteration processes and post-mining weathering on rock engineering properties of Goathill North rock pile at Questa mine, Taos County, New Mexico: M. S. thesis, New Mexico Institute of Mining and Technology, Socorro, 274 p., http://geoinfo.nmt.edu/staff/mclemore/Molycorppapers.htm, accessed December 06, 2007.

9. TECHNICAL APPENDICES

Boakye, B., 2008, Large In Situ Direct Shear Tests on Rock Piles At The Questa Mine, Taos County, New Mexico: M. S. thesis, New Mexico Institute of Mining and Technology, Socorro. http://geoinfo.nmt.edu/staff/mclemore/Molycorppapers.htm.

Fakhimi A., Boakye K., Sperling D., and McLemore V., 2008, Development of a modified in situ direct shear test technique to determine shear strength of mine rock piles, Geotechnical Testing Journal, v. 31, no. 3, paper on line www.astm.org

McLemore, V.T. and A. Dickens, 2008b, Petrographic Analysis, Mineralogy, and Chemistry of Samples Analyzed by In-Situ Direct Shear Methods, Questa, New Mexico: report to Chevron, Task B1.

APPENDIX 1. THE INPORTANCE OF NATURAL ANALOGS

Two natural analogs to weathering processes that occur in the rock piles are the debris flow and alteration scars. Lithology of the rock-pile material, debris flows, and alteration scars are similar and similar weathering processes are likely to occur in all three. Therefore, debris flows and alteration scars would provide an analog to mineralogical changes expected in the rock piles due to weathering. Table A1-1 summarizes some similarities and differences between these environments.

TABLE A1-1. Comparison of the different weathering environments in the rock piles and analog sites in the Questa area. See DRA-2, -19 and McLemore et al. (2008b) for more details. QSP=quartz-sericite-pyrite. SP=poorly-graded sand, GP=poorly-graded gravel, SM=silty sand, SC=clayey sand, GW=well-graded gravel, GC=clayey gravel, GP-GC=poorly-graded gravel with clay, GP-GM=poorly-graded gravel with silt, GW-GC=well-graded gravel with clay, SW-SC=well-graded sand with clay, SP-SC=poorly-graded sand with clay.

Feature	Rock Pile	Alteration Scar	Debris Flow
Rock types	Andesite Rhyolite Aplite Porphyry Intrusion	Andesite Rhyolite Aplite Porphyry Intrusion	Andesite Rhyolite Aplite Porphyry Intrusion
Unified soil classification (USCS)	GP-GC, GC, GP-GM, GW, GW-GC, SP-SC, SC, SW-SC, SM	GP-GC, GP	GP, SP, GP-GC
% fines	0.2-46 Mean 7.5 Std Dev. 6 No of Samples=89	0.6-20 Mean 5.2 Std Dev. 4 No of Samples=18	0.3-6 Mean 1.8 Std Dev. 2 No of Samples=12
Water content (%)	1-24 Mean 10 Std Dev. 4 No of Samples=390	1-20 Mean 9 Std Dev. 4 No of Samples=48	1-29 Mean 5 Std Dev. 4 No of Samples=36
Paste pH	1.6-9.9 Mean 4.8 std dev 1.9 No of samples=1368	2.0-8.3 Mean 4.3 std dev 1.6 No of samples=215	2.0-6.9 Mean 4.5 std dev 1.3 No of samples=58
Pyrite content (%)	Low to high 0-14% (mean 1.0%; std dev. 1.2%, No of samples=1098)	Low to high 0-11% (mean 0.7%, std dev 1.8%, No of samples=62)	Low to medium 0-0.2% (mean 0.03%, std dev 0.06%, No of samples=22)
Dry density kg/m^3	1400-2400 Mean 1800 Std Dev. 140 No of Samples=153	1500-2300 Mean 1900 Std Dev. 210 No of Samples=13	1300-2200 Mean 1900 Std Dev. 340 No of Samples=10
Particle shape	Angular to subangular to subrounded	Subangular	Subangular to subrounded

Feature	Rock Pile	Alteration Scar	Debris Flow
Plasticity Index (%)	0.2-20 Mean 10 Std Dev. 5 No of Samples=134	5-25 Mean 12 Std Dev. 5 No of Samples=30	3-14 Mean 7 Std Dev. 3 No of Samples=18
Degree of chemical cementation (visual observation)	Low to moderate (sulfates, Iron oxides)	Moderate to high (sulfates, Iron oxides)	Moderate to high (sulfates, Iron oxides)
Slake durability index (%)	80.9-99.5 Mean 96.6 Std Dev. 3.1 No of Samples=120	64.5-98.5 Mean 89.2 Std Dev. 9.2 No of Sample=24	96.1-99.6 Mean 98.4 Std Dev. 0.9 No of Samples=18
Point Load index (MPa)	0.6-8.2 Mean 3.8 Std Dev. 1.7 No of Samples=59	1.7-3.8 Mean 2.8 Std Dev. 0.8 No of Samples=4	2.6-6 Mean 4 Std Dev. 1 No of Samples=12
Peak friction angle (degrees), 2-inch shear box (NMIMT data)	35.3-49.3 Mean 42.2 Std Dev. 2.9 No of Samples=99	33.4-54.3 Mean 40.7 Std Dev. 4.8 No of Samples=22	39.2-50.1 Mean 44.3 Std Dev. 3.9 No of Samples=12
Average cohesion (kPa), in-situ shear tests	0-25.9 Mean 9.6 Std dev 7.3 No of samples=20	12.1-23.9 Mean 18.1 No of samples=2	31.4-46.1 Mean 38.8 No of samples=2

In-situ test sites were chosen in the Goat Hill debris flow and Questa Pit alteration scar in order to test this hypothesis. The two sites are somewhat different in physical characteristics and depositional processes, as explained in McLemore and Dickens (2008a), Ayakwah et al. (2008) and summarized below.

The debris flow consists of several different flows or landslides of material that washed out of the Goat Hill alteration scar upstream during heavy rainfall events. Water was a mechanism of deposition. However, the debris flows represent some of the best cemented material in the area and the in-situ tests were designed to examine that cementation. The in-situ tests were conducted in the forest at the top of a road cut into the debris slope. Ayakwah et al. (2008) describes the Goat Hill debris flow in more detail.

The in-situ site within the Questa Pit alteration scar was selected in a talus or scree deposit of rock fall or landslide material that formed when the natural slope of the scar slid, possibly as a result of heavy rainfall. This material was deposited in a similar fashion to the rock piles, in that the material most likely was largely rocks and soil that slid due to gravity and was deposited similar to end-dumping of rock pile material. There was likely water involved in the failure, but mostly the material failed as a result of gravity. The in-situ tests were conducted on a bench cut into the scree slope.

APPENDIX 2. WEATHERING INDICES

The evidence for weathering in the Questa rock piles includes (McLemore et al., 2006a, b, 2008a):

- Change in color from darker brown and gray in less weathered samples (original color of igneous rocks) to yellow to white to light gray in the weathered samples
- Thin yellow to orange, “burnt” layers within the interior of GHN, where water and/or air flowed and oxidized the rock pile material
- Paste pH, in general, is low in oxidized, weathered samples and paste pH is higher in less weathered samples

- Presence of jarosite, gypsum, iron oxide minerals and Fe soluble salts (often as cementing minerals), and low abundance to absence of calcite, pyrite, and epidote in weathered samples
- Tarnish or coatings of pyrite surfaces within weathered samples
- Dissolution textures of minerals (skeletal, boxwork, honeycomb, increase in pore spaces, fractures, change in mineral shape, accordion-like structures, loss of interlocking textures, pits, etching) within weathered samples (McLemore et al., 2008a)
- Chemical classification as potential acid-forming materials using acid base accounting methods (Tachie-Menson, 2006)
- Chemical analyses of water samples characterized by acidic, high sulfate, high TDS, and high metal concentrations (Al, Ca, Mg, Fe, Mn, SO_4).

In GHN, typically, paste pH increased with distance from the outer, oxidized units (west) towards the interior units (east) of the GHN rock pile. The outer units were oxidized (weathered) based upon the white and yellow coloration, low paste pH, presence of jarosite and authigenic gypsum, and absence of calcite. The base of the rock pile adjacent to the bedrock/colluvium surface represents the oldest part of the rock pile because it was laid down first. Portions of the base appeared to be nearly or as oxidized (weathered) as the outer, oxidized zone of the rock pile. This suggests that air and water flowed along the basal interface, implying that it could have been an active weathering zone.

A simple weathering index (SWI) was developed to differentiate the weathering intensity of Questa rock pile materials (SWI=1, fresh to SWI=5, most weathered; Table A2-1; Gutierrez et al, 2008). The following 5 classes (Table A2-1) describes the SWI classification for the mine soils at the Questa mine based on relative intensity of both physical and chemical weathering (modified in part from Little, 1969; Gupta and Rao, 1998; Blowes and Jambor, 1990):

1. Fresh
2. Least weathered
3. Moderately weathered
4. Weathered
5. Highly weathered

TABLE A2-1. Simple weathering index for rock-pile material (including rock fragments and matrix) at the Questa mine.

SWI	Name	Description
1	Fresh	Original gray and dark brown to dark gray colors of igneous rocks; little to no unaltered pyrite (if present); calcite, chlorite, and epidote common in some hydrothermally altered samples. Primary igneous textures preserved.
2	Least weathered	Unaltered to slightly altered pyrite; gray and dark brown; very angular to angular rock fragments; presence of chlorite, epidote and calcite, although these minerals not required. Primary igneous textures still partially preserved.
3	Moderately weathered	Pyrite altered (tarnished and oxidized), light brown to dark orange to gray:, more clay- and silt-size material; presence of altered chlorite, epidote and calcite, but these minerals not required. Primary igneous textures rarely preserved.
4	Weathered	Pyrite very altered (tarnished, oxidized, and pitted); Fe hydroxides and

		oxides present; light brown to yellow to orange; no calcite, chlorite, or epidote except possibly within center of rock fragments (but the absence of these minerals does not indicate this index), more clay-size material. Primary igneous textures obscured.
5	Highly weathered	No pyrite remaining; Fe hydroxides and oxides, shades of yellow and red typical; more clay minerals; no calcite, chlorite, or epidote (but the absence of these minerals does not indicate this index); angular to subrounded rock fragments

The SWI accounts for changes in color, texture, and mineralogy due to weathering, but it is based on field descriptions. Some problems with this weathering index are:

- It is subjective and based upon field observations.
- This index does not always enable distinction between pre-mining supergene hydrothermal alteration and post-mining weathering.
- The index is developed from natural soil profiles, which weathered differently from the acidic conditions within the Questa rock piles and, therefore, this index may not adequately reflect the weathering conditions within the rock piles.
- This index refers mostly to the soil matrix; most rock fragments within the sample are not weathered except perhaps at the surface of the fragment and along cracks.
- The index is based primarily upon color and color could be indicative of other processes besides weathering intensity.
- This index was developed for the Questa rock piles and may not necessarily apply to other rock piles.
- Weathering in the Questa rock piles is an open not a closed system (i.e. water analysis indicates the loss of cations and anions due to oxidation).

Paste pH is another indication of weathering used in this project, but it too has limitations. Paste pH is the pH measured on a paste or slurry that forms upon mixing soil material and deionized water. In an acidic material, paste pH is an approximate measurement of the acidity of a soil material that is produced by the oxidation of pyrite and other sulfides. A low paste pH (2-3) along with yellow to orange color and the presence of jarosite, gypsum, and low abundance to absence of calcite is consistent with oxidized conditions in the Questa rock piles (McLemore et al., 2006a, b; Gutierrez et al., 2008). In general, paste pH increases from the outer, oxidized portion of GHN to the inner, less oxidized portion.

The in-situ samples were chemically evaluated using acid base accounting methods (using procedures described by Tachie Menson, 2006). Most in-situ samples are potentially acid forming and represent weathered material (Fig. A2-1).

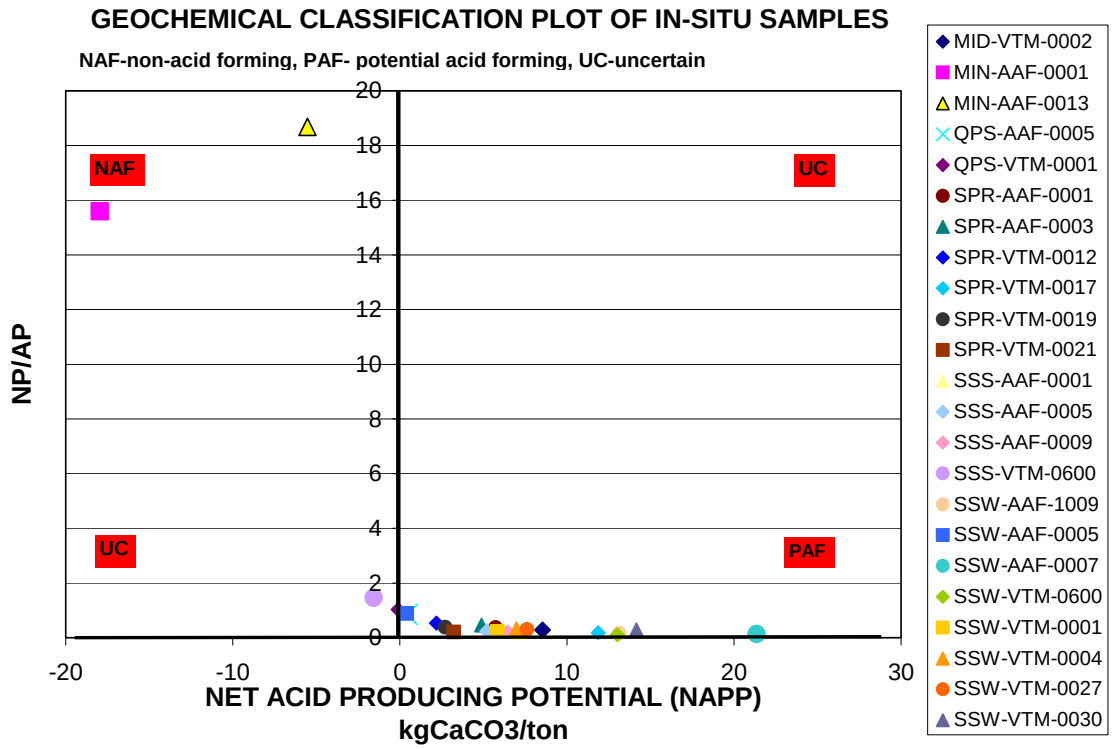

FIGURE A2-1. Chemical classification chart of in-situ samples. Most samples are potentially acid forming and represent weathered material. Non-acid forming samples are not significantly weathered.

The Questa Mineralogical Weathering Index was developed specifically for the Questa rocks and is based upon the pyrite-calcite to gypsum-jarosite system and includes some dissolution of silicates (Fig. A2-2).

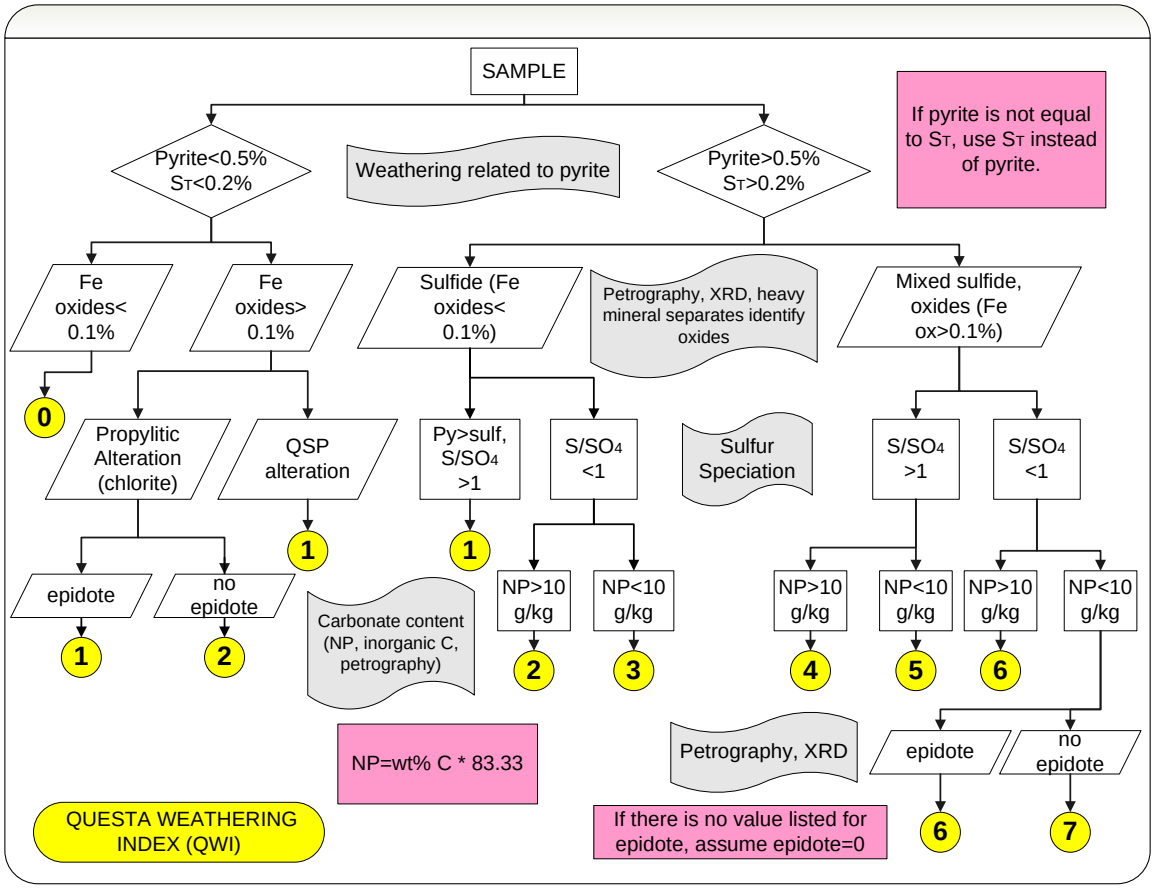

FIGURE A2-2. Decision tree for determining the Questa Mineralogical Weathering Index (QMWI).

APPENDIX 3. FIGURES AND TABLES.

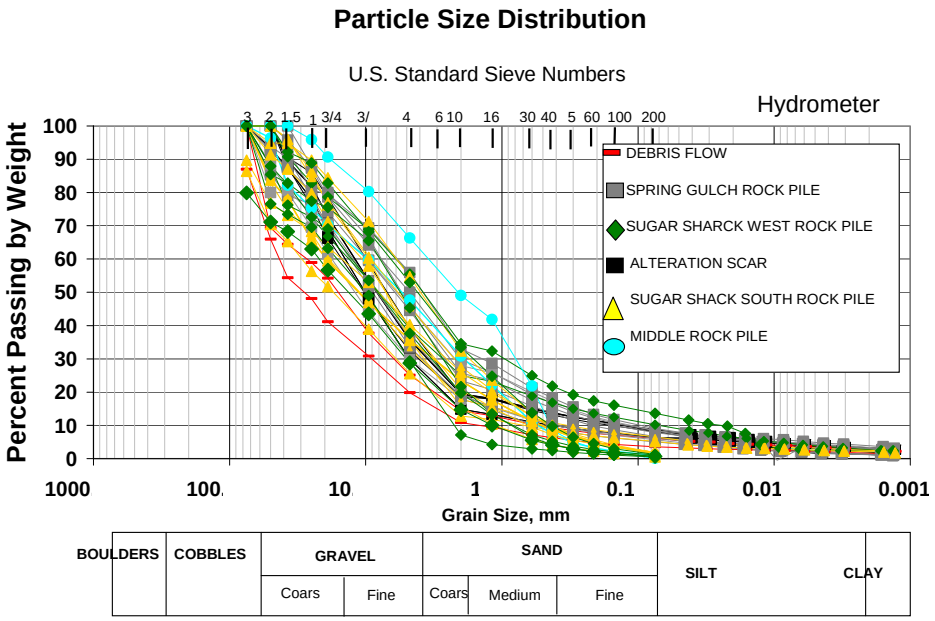

FIGURE A3-1. Gradation curves of the rock pile materials collected from the locations where in-situ shear tests were conducted.

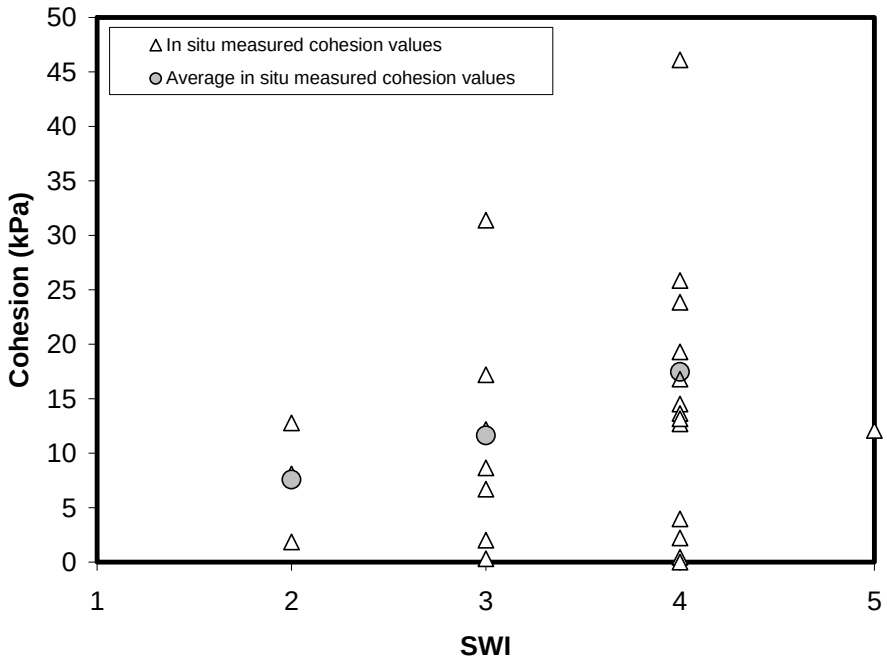

FIGURE A3-2. Scatter plot of cohesion versus simple weathering index (SWI).

TABLE A3-1. Some of the geotechnical properties of rock piles and analogs, and the descriptive statistics of field cohesion values, grouped according to the SWI.

Rock piles and Analogs	**Test id**	**Matric Suction (kPa)**	**Fine (%)**	**PI (%)**	**USCS**	**SWI**	**Field Cohesion (kPa)**	**No. of Tests**	**Cohesion (kPa)**	
									Mean	**STD**
Sugar Shack South Rock Pile	SSS-VTM-0600-1	1	6.9	8.7	GP-GC	2	1.9	**3**	**7.6**	**5.5**
Spring Gulch Rock Pile	SPR-AAF-0001-1	10	1.3	1.4	GP	2	8.1			
Spring Gulch Rock Pile	SPR-AAF-0001-2	9	0.6	9.5	GP	2	12.8			
Sugar Shack South Rock Pile	SSS-AAF-0001-1	1	1.8	7.3	GP	3	6.7	**7**	**11.2**	**10.6**
Sugar Shack South Rock Pile	SSS-AAF-0005-1	9	1.4	4.7	SP	3	17.2			
Sugar Shack South Rock Pile	SSS-AAF-0009-1	0	2.0	10.5	GP	3	2.0			
Sugar Shack West Rock Pile	SSW-AAF-0004-1	n/a	13.6	14.2	GP-GC	3	8.7			
Sugar Shack West Rock Pile	SSW-VTM-0026-1	13	0.7	4.2	SP	3	0.3			
Sugar Shack West Rock Pile	SSW-VTM-0030-1	3	0.7	7.1	GP	3	12.2			
Debris Flow	MIN-AAF-0001-1	25	3.6	3.6	GP	3	31.4			
Middle Rock Pile	MID-VTM-0002-1	1	1.0	1.9	GP	4	0.5	**13**	**14.8**	**12.6**
Debris Flow	MIN-AAF-0012-1	31	0.7	8.9	GP	4	46.1			
Sugar Shack West Rock Pile	SSW-AAF-0005-1	5	2.9	8.2	GP	4	25.9			
Sugar Shack West Rock Pile	SSW-AAF-0007-1	9	0.6	7.2	SP	4	13.2			
Sugar Shack West Rock Pile	SSW-VTM-0600-1	n/a	0.2	7.7	GP	4	19.3			
Sugar Shack West Rock Pile	SSW-VTM-0600-2	n/a	1.5	6.2	GP	4	13.6			
Sugar Shack West Rock Pile	SSW-VTM-0600-3	n/a	13.6	9.2	GC	4	2.2			
Spring Gulch Rock Pile	SPR-VTM-0012-1	2	8.4	2.5	GP-GM	4	12.7			
Spring Gulch Rock Pile	SPR-VTM-0012-2	0	6.7	6.2	GP-GC	4	4.0			
Spring Gulch Rock Pile	SPR-VTM-0012-3	0	7.9	4.3	GP-GC	4	0.0			
Spring Gulch Rock Pile	SPR-VTM-0019-1	5	10.0	7.3	SP-SC	4	14.5			
Spring Gulch Rock Pile	SPR-VTM-0019-2	2	8.5	6.9	GP-GC	4	16.8			
Questa Pit Alteration Scar	QPS-AAF-0001-3	0	6.8	16.4	GP-GC	4	23.9			
Questa Pit Alteration Scar	QPS-VTM-0001-1	11	4.2	5.3	GP	5	12.1	**1**		

TABLE A3-2. Descriptive statistics of field cohesion of the rock piles and analogs, reported separately. Only test results on the shear blocks that had rock fragments less than one fifth of the box width are reported in this table.

State	**Cohesion (kPa)**		
	Mean	**STD**	**No. of *in situ* tests**
Rock piles at the placement time	0	0	N/A
Rock piles after 25-40 years (current situation)	9.6	7.3	20
Analogs (thousands of years old)	28.4	14.2	4

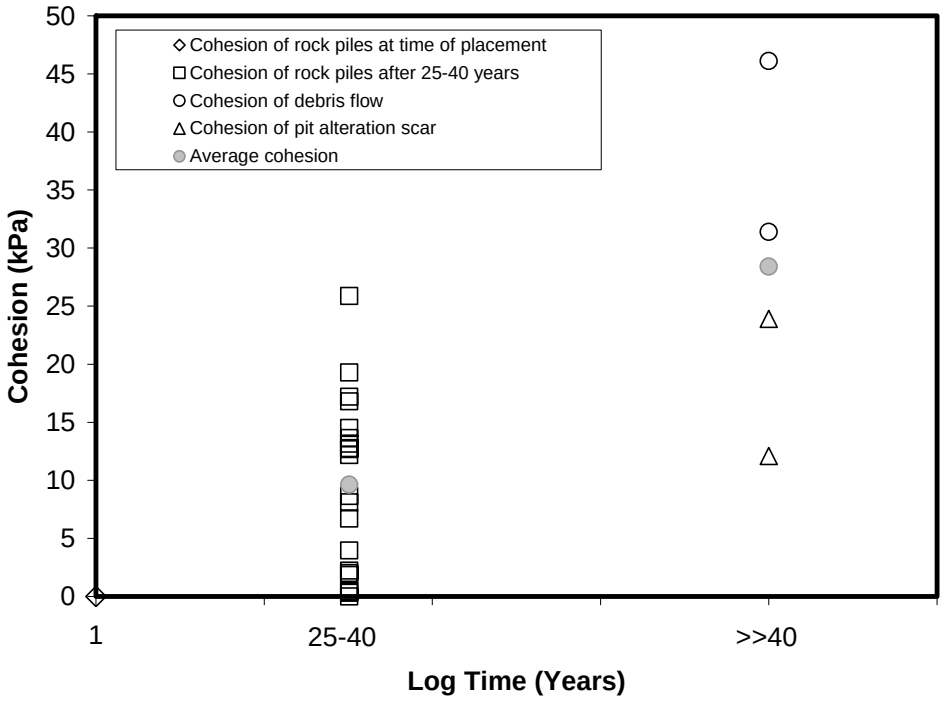

FIGURE A3-3. Cohesion vs. age of the rock piles and analogs.

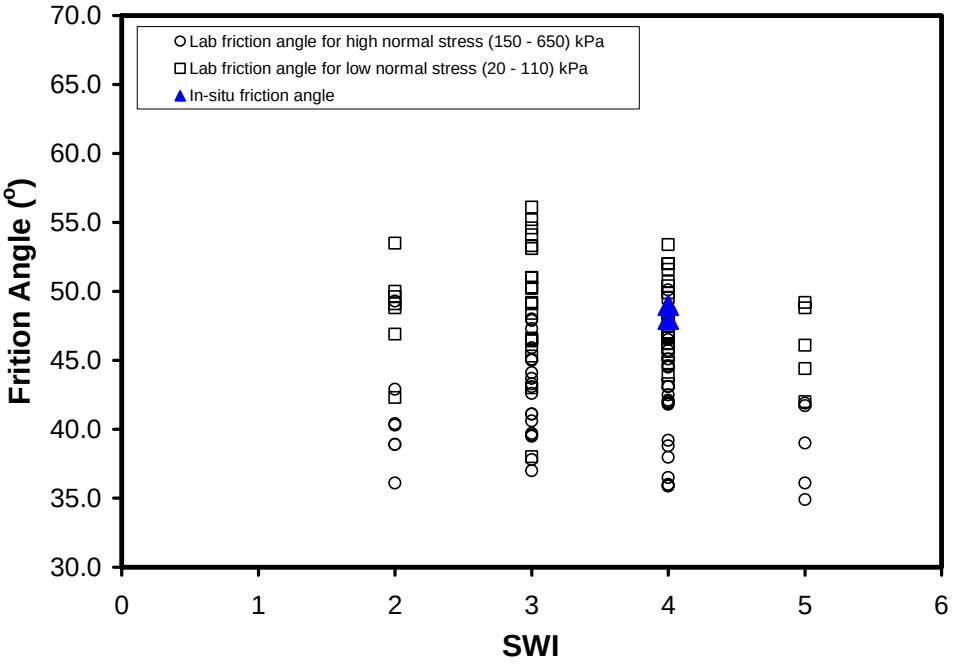

FIGURE A3-4. In situ and laboratory friction angles versus simple weathering index (SWI).

TABLE A3-3. In situ dry density and the corresponding dry density that each sample was compacted in the laboratory for the direct shear tests. The gray-highlighted rows indicate the samples with the compacted laboratory dry densities within (0.95 to 1.05) of the corresponding in situ dry densities.

Sample id	laboratory dry density (kg/m3)	In-situ dry density (kg/m3)
QPS-AAF-0001 (QPS-AAF-0001-1)	1650	1680
QPS-AAF-0003 (QPS-AAF-0001-2)	1860	1880
QPS-AAF-0005 (QPS-AAF-0001-3)	1670	1660
QPS-AAF-0008 (QPS-AAF-0008-1)	1520	1510
QPS-AAF-0009 (QPS-AAF-0009-1)	1970	1920
QPS-AAF-0020 (QPS-AAF-0020-1)	1950	1960
QPS-AAF-0022 (QPS-AAF-0022-1)	1860	1860
QPS-VTM-0001 (QPS-VTM-0001-1)	1840	n/a
MIN-AAF-0001 (MIN-AAF-0001-1)	1850	2460
MIN-AAF-0010 (MIN-AAF-0010-1)	2030	2080
MIN-AAF-0012 (MIN-AAF-0012-1)	1880	n/a
MIN-AAF-0015 (MIN-AAF-0015-1)	1980	1940

Sample id	laboratory dry density (kg/m3)	In-situ dry density (kg/m3)
MIN-AAF-0004 (MIN-AAF-0004-1)	1830	1890
MID-AAF-0001 (MID-AAF-0001-1)	1880	n/a
MID-VTM-0001 (MID-AAF-0002-1)	1960	2120
MID-AAF-0002 (MID-AAF-0002-2)	1960	2120
MID-VTM-0002 (MID-VTM-0002-1)	2160	2680
SPR-AAF-0001 (SPR-AAF-0001-1(1))	1830	1830
SPR-AAF-0003 (SPR-AAF-0001-2)	2170	2160
SPR-VTM-0005 (SPR-VTM-0005-1)	1570	1570
SPR-VTM-0008 (SPR-VTM-0008-1)	1900	1880
SPR-VTM-0010 (SPR-VTM-0008-2)	1460	1430
SPR-VTM-0012 (SPR-VTM-0012-1)	1830	1970
SPR-VTM-0014 (SPR-VTM-0012-2)	1500	n/a
SPR-VTM-0017 (SPR-VTM-0012-3)	1920	n/a
SPR-VTM-0019 (SPR-VTM-0019-1)	1680	1670
SPR-VTM-0021 (SPR-VTM-0019-2)	1620	1600
SSS-AAF-0001 (SSS-AAF-0001-1)	1940	1940
SSS-AAF-0004 (SSS-AAF-0001-2)	1810	n/a
SSS-AAF-0005 (SSS-AAF-0005-1)	1910	1920
SSS-AAF-0007 (SSS-AAF-0005-2)	1890	1850
SSS-AAF-0009 (SSS-AAF-0009-1)	1930	1810
SSS-AAF-0013 (SSS-AAF-0009-2)	1960	2090
SSS-VTM-0600 (SSS-VTM-0600-1)	1840	1860
SSS-VTM-0601 (SSS-VTM-0601-1)	1840	n/a
SSW-AAF-0001 (SSW-AAF-0001-1)	1820	1780
SSW-AAF-0002 (SSW-AAF-0002-1)	1670	n/a
SSW-AAF-1002 (SSW-AAF-0002-2)	1670	n/a
SSW-AAF-1005 (SSW-AAF-0002-3)	1670	1870
SSW-AAF-0005 (SSW-AAF-0005-1)	1760	1730
SSW-AAF-0007 (SSW-AAF-0007-1)	1860	1860
SSW-AAF-0004 (SSW-AAF-0004-1)	1840	n/a
SSW-VTM-0016 (SSW-VTM-0016-1)	2000	2090
SSW-AAF-0019 (SSW-VTM-0016-2)	2040	2430
SSW-VTM-0023 (SSW-VTM-0023-1)	2080	2200
SSW-AAF-0027 (SSW-VTM-0026-1)	1980	2040
SSW-VTM-0028 (SSW-VTM-0026-2)	2020	2300
SSW-VTM-0030 (SSW-VTM-0030-1)	2110	2120
SSW-VTM-0032 (SSW-VTM-0030-2)	2100	2110
SSW-VTM-0600 (SSW-VTM-0600-1)	1410	1410
SSW-VTM-0001 (SSW-VTM-0600-2)	1750	1660
SSW-VTM-0004 (SSW-VTM-0600-3)	1800	1900

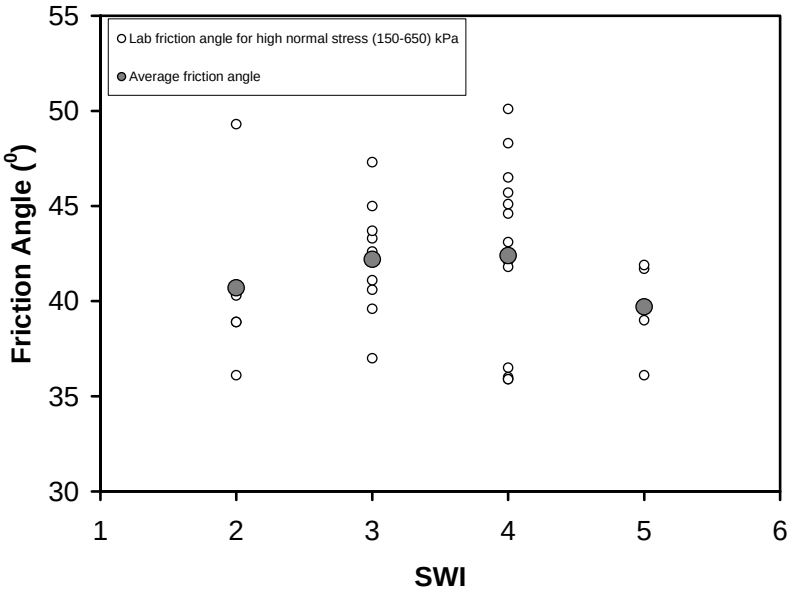

FIGURE A3-5. Laboratory friction angles versus simple weathering index (SWI) for the 32 samples compacted to the dry densities within 0.95 to 1.05 of the corresponding in situ dry densities.

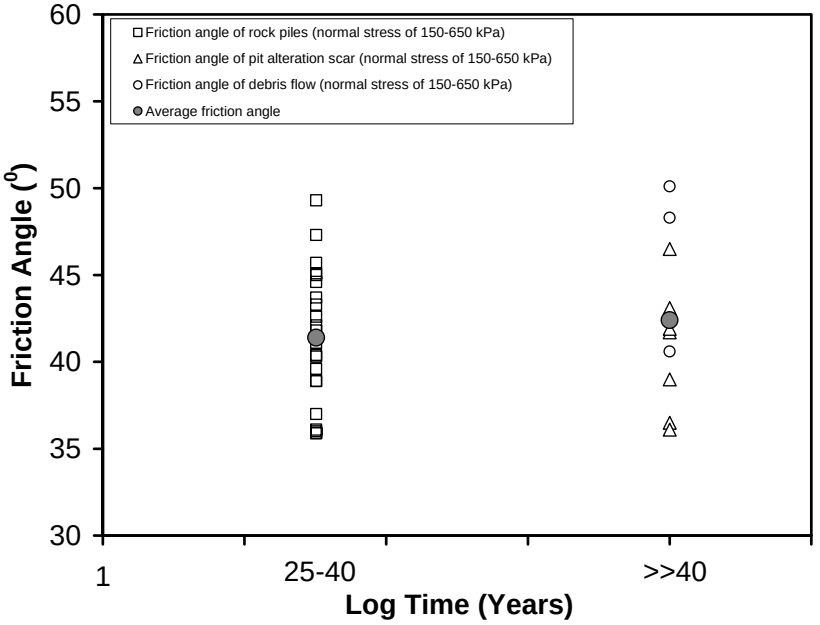

FIGURE A3-6. Laboratory friction angle versus age for the 32 samples compacted to the dry densities within 0.95 to 1.05 of the corresponding in situ dry densities.

FIGURE A3-7. A close photo of the surface of a Questa rock pile material showing the angularity of the rock fragments compared to a spherical ball 50 mm in diameter.

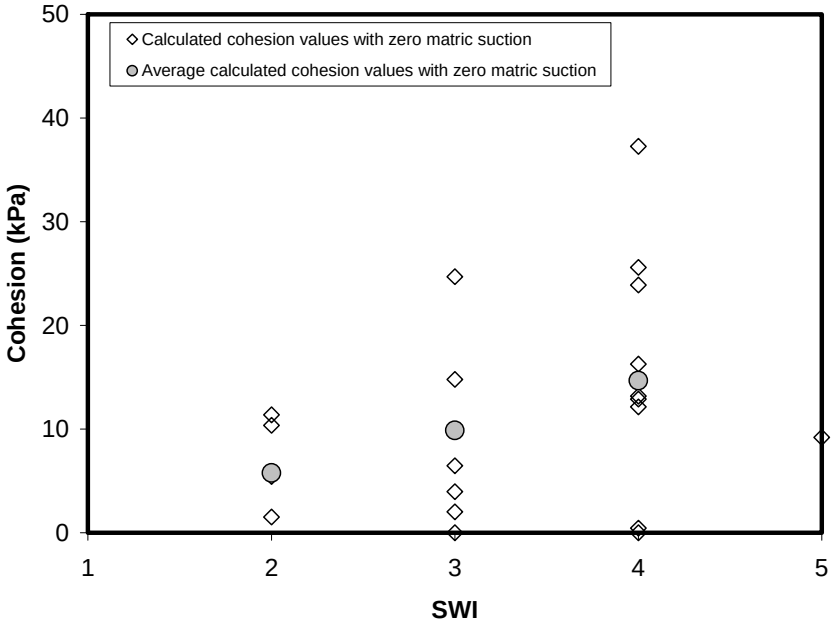

FIGURE A3-8. Scatter plot of cohesion corresponding to when the cohesion values are adjusted for matric suction equal to 0 kPa (c' in equation 1b) vs. the simple weathering index (SWI).

APPENDIX 4. Statistical Analyses for Cohesion

Hypothesis. The cohesion (kPa) of the Questa rock piles, alteration scars and debris flows is different.

Data. Data are results obtained from NMT sampling and testing on Questa rock piles and analogs in 2006-2007 (Table A4-1).

TABLE A4-1. Cohesion (kPa) measurements by NMT 2006-2007.

Questa rock piles	Alteration scars	Debris flows
0.5	23.9	31.4
8.1	12.1	46.1
12.8		
12.7		
4.0		
0.0		
14.5		
16.8		
6.7		
17.2		
2.0		
1.9		
25.9		
13.2		
8.7		
0.3		
12.2		
19.3		
13.6		
2.2		

Approach. Histograms are below. The tests were conducted using the SigmaStat@ software. The normality test (assumption that they were drawn from a normal population) passed (P=0.197) and the equal variance test (assumption that the samples were drawn from populations with the same variance) passed (P=0.900), so the one way ANOVA (Analysis of Variance) was used. F is the statistic. If the F ratio is around 1, you can conclude that there are no significant differences between groups (i.e., the data groups are consistent with the null hypothesis that all the samples were drawn from the same population). If F is a large number, you can conclude that at least one of the samples was drawn from a different population (i.e., the variability is larger than what is expected from random variability in the population). To determine exactly which groups are different, examine the multiple comparison results. The P value is the probability of being wrong in concluding that there is a true difference between the groups. The power, or sensitivity, of a One Way ANOVA is the probability that the test will detect a difference among the groups if there really is a difference. The closer the power is to 1, the more sensitive the test. Alpha is the acceptable probability of incorrectly concluding that there is a difference. The alpha value is set in the Options for One Way ANOVA dialog; the suggested value is $\alpha = 0.05$ which indicates that a one in twenty chance of error is acceptable. Smaller values of a result in stricter requirements before concluding there is a significant difference, but a greater possibility of concluding there is no

difference when one exists (a Type II error). Larger values of α make it easier to conclude that there is a difference but also increase the risk of seeing a false difference (a Type I error).

Results. The results in kPa are summarized in Table A4-2. SEM=standard error of the mean, DF=degrees of freedom, SS=sum of squares.

Table A4-2. Results of statistical test.

Group Name	Number	Missing	Mean	Standard Deviation	SEM
alteration scar	2	0	18.000	8.344	5.900
debris flow	2	0	38.750	10.394	7.350
rock piles	20	0	9.630	7.345	1.642

Source of Variation	DF	SS	MS	F	P
Between Groups	2	1601.813	800.906	13.984	<0.001
Residual	21	1202.707	57.272		
Total	23	2804.520			

Power of performed test with alpha = 0.050 is 0.995.

Conclusion. The differences in the mean values among the treatment groups are greater than would be expected by chance; there is a statistically significant difference in cohesion between the alteration scar, debris flow, and Questa rock piles (P = <0.001).

HISTOGRAMS